IEIE Transactions on Smart Processing and Computing, vol. 4, no. 4, August 2015
http://dx.doi.org/10.5573/IEIESPC.2015.4.4.195

Median Filtering Detection of Digital Images Using Pixel Gradients

Kang Hyeon RHEE

Dept. of Electronics Eng. and School of Design and Creative Eng., Chosun University / Gwangju 501-759, Korea
khrhee@chosun.ac.kr

***** Corresponding Author:

Received July 15, 2015; Revised August 5, 2015; Accepted August 24, 2015; Published August 31, 2015

** Short Paper: This paper is invited by Seung-Won Jung, the associate editor.*

** Extended from a Conference: Preliminary results of this paper were presented at the ITC-CSCC 2015. The present paper has been accepted by the editorial board through the regular reviewing process that confirms the original contribution.*

***Abstract*:** For median filtering (MF) detection in altered digital images, this paper presents a new feature vector that is formed from autoregressive (AR) coefficients via an AR model of the gradients between the neighboring row and column lines in an image. Subsequently, the defined 10-D feature vector is trained in a support vector machine (SVM) for MF detection among forged images. The MF classification is compared to the median filter residual (MFR) scheme that had the same 10-D feature vector. In the experiment, three kinds of test items are area under receiver operating characteristic (ROC) curve (AUC), classification ratio, and minimal average decision error. The performance is excellent for unaltered (ORI) or once-altered images, such as 3×3 average filtering (AVE3), QF=90 JPEG (JPG90), 90% down, and 110% up to scale (DN0.9 and Up1.1) images, versus 3×3 and 5×5 median filtering (MF3 and MF5, respectively) and MF3 and MF5 composite images (MF35). When the forged image was post-altered with AVE3, DN0.9, UP1.1 and JPG70 after MF3, MF5 and MF35, the performance of the proposed scheme is lower than the MFR scheme. In particular, the feature vector in this paper has a superior classification ratio compared to AVE3. However, in the measured performances with unaltered, once-altered and post-altered images versus MF3, MF5 and MF35, the resultant AUC by 'sensitivity' (TP: true positive rate) and '1-specificity' (FN: false negative rate) is achieved closer to 1. Thus, it is confirmed that the grade evaluation of the proposed scheme can be rated as '*Excellent* (*A*)'.

***Keywords*:** Forgery image, Median filtering (MF), Median filtering detection, Median filter residual (MFR), Median filtering forensic, Autoregressive (AR) model, Pixel gradient

1. Introduction

In image alteration, content-preserving manipulation uses compression, filtering, averaging, rotation, mosaic editing and scaling, and so on, using the forgery method [1-4]. Median filtering (MF) is especially preferred among some forgers because it has characteristics of non-linear filtering based on order statistics. Furthermore, the MF detection technique could classify altered images by MF. The state of the art is well-documented [5-9]. Consequently, an MF detector becomes a significant forensic tool for recovery of the processing history of a forged image.

To detect MF in a forged image, Cao *et al*. [10] analyzed the probability that an image's first-order pixel difference is zero in textured regions. In this regard, Stamm *et al*. [2] accounted for a method that is highly accurate with unaltered or uncompressed images.

Meanwhile, to extract the feature vector for median filtering detection, Kang *et al*. [6] obtained autoregressive (AR) coefficients as feature vectors via an AR model to analyze the median filter residual (MFR), which is the difference values of the original and its median filtering image.

In this paper, a new MF detection algorithm is proposed in which the feature vector is formed from AR coefficients via an AR model of the gradients of the

neighboring horizontal and vertical lines in an image.

The rest of the paper is organized as follows. Section 2 briefly introduces the theoretical background of MFR, and a gradient of the neighboring lines in an image. Section 3 describes the extraction method of a new feature vector in the proposed MF detection algorithm. The experimental results of the proposed algorithm are shown in Section 4. The performance evaluation is compared to a previous one, and is followed by some discussion. Finally, the conclusion is drawn, and future work presented in Section 5.

2. Theoretical Background

In this section, the MFR and a gradient of the neighboring lines in an image are briefly introduced.

2.1 MFR

Kang *et al.* proposed a MFR [6] that used a 10-D feature vector, which computed AR coefficients of the difference values between the original image (y) and its median filtering image (med(y)). Yuan [7] attempted to reduce interference from an image's edge content and block artifacts from JPEG compression, proposing to gather detection features from an image's MFR.

The difference values (d) between the original and its median filtering image are AR-modeled. The difference is referred to as the median filter residual, which is formally defined as

$$\begin{aligned} d(i,j) &= \mathrm{med}_w\left(y(i,j)\right) - y(i,j) \\ &= z(i,j) - y(i,j) \end{aligned} \quad (1)$$

where (i,j) is a pixel coordinate, and w is the MF window size ($w \in \{3,5\}$). AR coefficients a_k are computed as

$$a_k^{(r)} = \mathrm{AR}\left(\mathrm{mean}\left(d^{(r)}\right)\right) \quad (2)$$

$$a_k^{(c)} = \mathrm{AR}\left(\mathrm{mean}\left(d^{(c)}\right)\right) \quad (3)$$

$$a_k = \left(a_k^{(r)} + a_k^{(c)}\right)/2 . \quad (4)$$

where r and c are the row and column directions, k is the AR order number, and $a_k^{(r)}$ and $a_k^{(c)}$ are the AR coefficients in the row and column directions, respectively. Then a single a_k for a one-dimensional AR model is obtained from Eq. (4), for which the average AR coefficients in both directions are Eqs. (2) and (3).

The author attempts to reduce the dimensionality of the feature vector according to an image's statistical property, fitting the MFR to a one-dimensional AR model in the row direction:

$$d(i,j) = -\sum_{q=1}^{p} a_k^{(r)} d(i,j-q) + \varepsilon^{(r)}(i,j), \quad (5)$$

and in the column direction:

$$d(i,j) = -\sum_{q=1}^{p} a_k^{(c)} d(i-q,j) + \varepsilon^{(c)}(i,j), \quad (6)$$

where $\varepsilon^{(r)}(i,j)$ and $\varepsilon^{(c)}(i,j)$ are the prediction errors [11], and p refers to the order of the AR model. Again, AR coefficients are the difference image (d).

2.2 Gradient of Neighboring Lines in Image

The gradients of the neighboring row and column direction lines in an image (x) are defined as $G^{(r)}$ and $G^{(c)}$ respectively as follows:

$$G^{(r)}(i,j) = x(i,j+1) - x(i,j) \quad (7)$$

$$G^{(c)}(i,j) = x(i+1,j) - x(i,j) \quad (8)$$

3. The Proposed MF Detection Algorithm

For the proposed MF detection algorithm, AR coefficients are computed via an AR model with Eqs. (7) and (8), then Eqs (9) and (10) as follows:

$$g_k^{(r)} = AR\left(\mathrm{mean}\left(G^{(r)}\right)\right) \quad (9)$$

$$g_k^{(c)} = AR\left(\mathrm{mean}\left(G^{(c)}\right)\right) . \quad (10)$$

$$g_k = \left(g_k^{(r)} + g_k^{(c)}\right)/2 . \quad (11)$$

In Eq. (11), g_k [1^{st}:10^{th}] is formed as a 10-D feature vector. The flow diagram of the proposed algorithm for MF detection is shown in Fig. 1.

The MF detection algorithm is described in the following steps, and is presented in Fig. 2.

[Step 1] Compute the neighboring row and column line gradients in the image.

[Step 2] Build the AR model of Step 1's gradients.

[Step 3] In Step 2, AR coefficients [1^{st} :10^{th}] of the gradients are formed as a 10-D feature vector.

[Step 4] The feature vector is trained in an SVM classifier.

[Step 5] Implement the MF detector via the trained SVM.

4. Performance Evaluation

The proposed scheme uses C-SVM with Gaussian kernel (12) with a 10-D feature vector.

$$K(x_i, x_j) = \exp\left(-\gamma \left\| x_i - x_j \right\|^2\right) \quad (12)$$

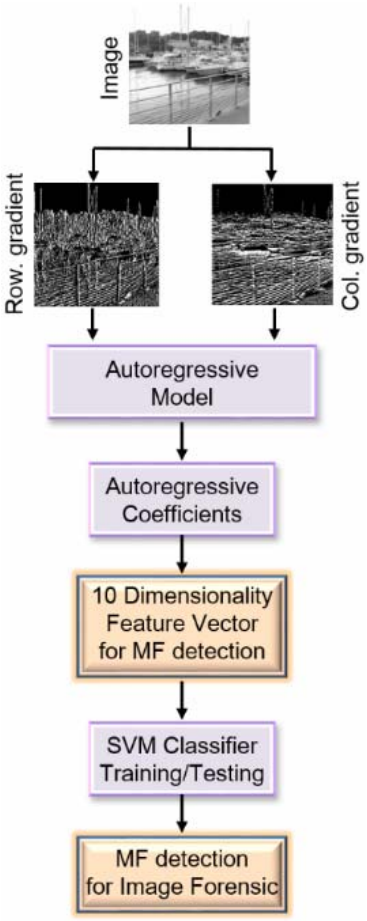

Fig. 1. The flow diagram of the proposed MF detection algorithm.

Main Median Filtering detection

Begin Feature Vector Extraction
Gradients ← Neighboring Row and Col. Lines in Image.
Feature Vector ← *AR_Model*(Gradients).
End Feature Vector Extraction

Begin Training Feature Vector
SVM Classifier (Feature Vector).
End Training Feature Vector

Begin Test Images
Feature Vectors of Test Images → Trained SVM Classifier.
End Test Images

Begin Classification and Analysis
Score, Classification and Confusion Table by Trained SVM Classifier.
Median Filtering Decision ← Analyze Confusion Table.
End Classification and Analysis

Leave Median Filtering detection

Fig. 2. Proposed MF detection.

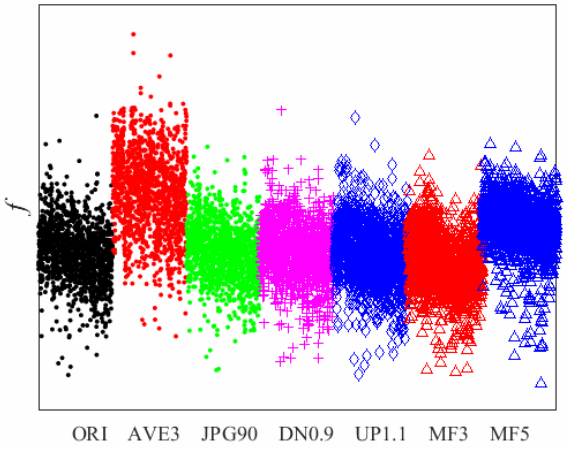

Fig. 3. The feature vector distribution of the MFR.

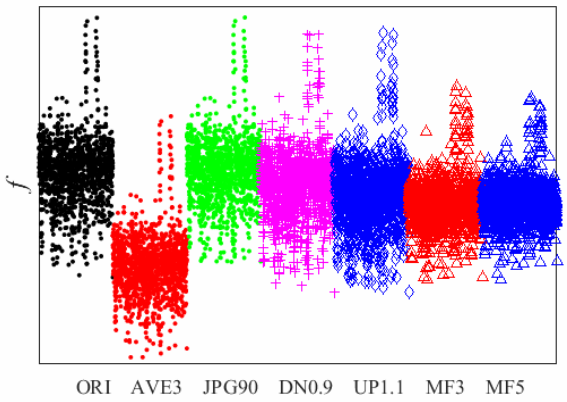

Fig. 4. The feature vector distribution of the proposed MF detection.

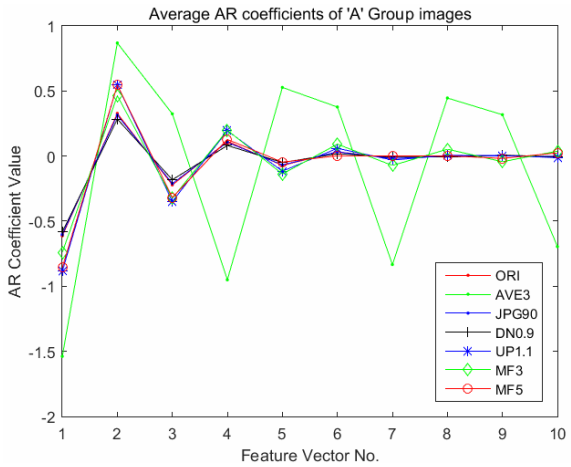

Fig. 5. Average AR coefficients of 'A' group images of the proposed MF detection scheme.

and a formed 10-D feature vector to an SVM classifier with trained five-fold cross-validation in conjunction with a grid search for the best parameters of C and γ in the multiplicative grid.

$$(C,\gamma) \in \left\{ \left(2^i, 2^j\right) \mid 4\times i, 4\times j \in Z \right\} \tag{13}$$

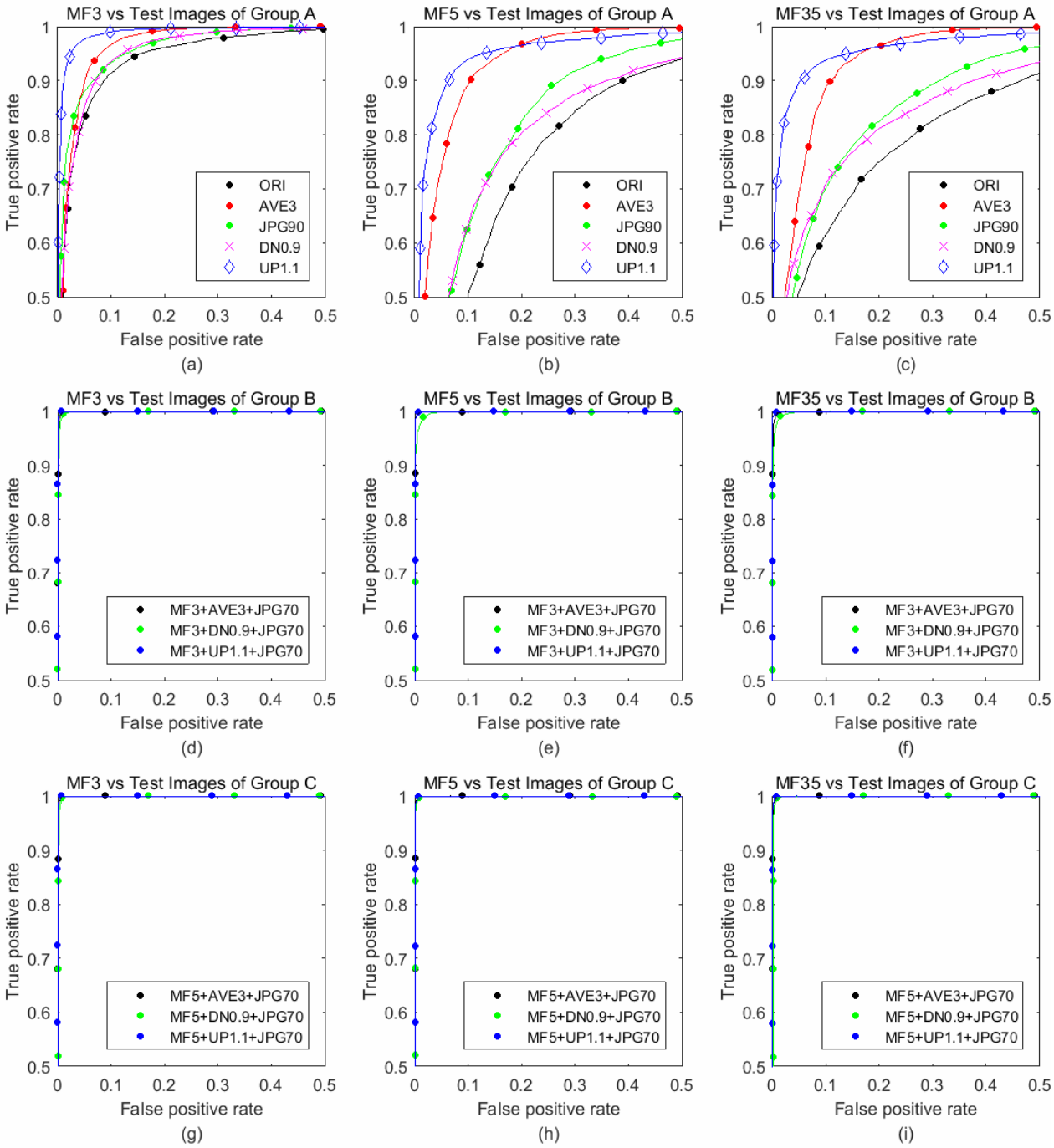

Fig. 6. ROC curves of MFR [7] scheme.

The searching step size for i,j is 0.25, and those parameters are used to get the classifier model on the training set.

UCID (Uncompressed Color Image Database)'s 1,388-image database (DB) [12] is used for MF detection, and test image types prepared were MF3, MF5, unaltered (ORI), 3×3 average filtering (AVE3), JPEG (QF=90) and 90% down and 110% up to scale (DN0.9 and UP1.1).

Subsequently, the trained classifier model was used to perform classification on the testing set. From among UCID's

1,388-image DB, 1,000 images were randomly selected for training, and the other 388 images were allocated to testing.

In Figs. 3 and 4, the feature vector distributions of the MFR and the proposed MF detection scheme, respectively, are presented.

The test image group was prepared with three kinds:

• Group A: the unaltered and the once-altered images.
- ORI
- AVE3
- JPG90
- DN0.9
- UP1.1

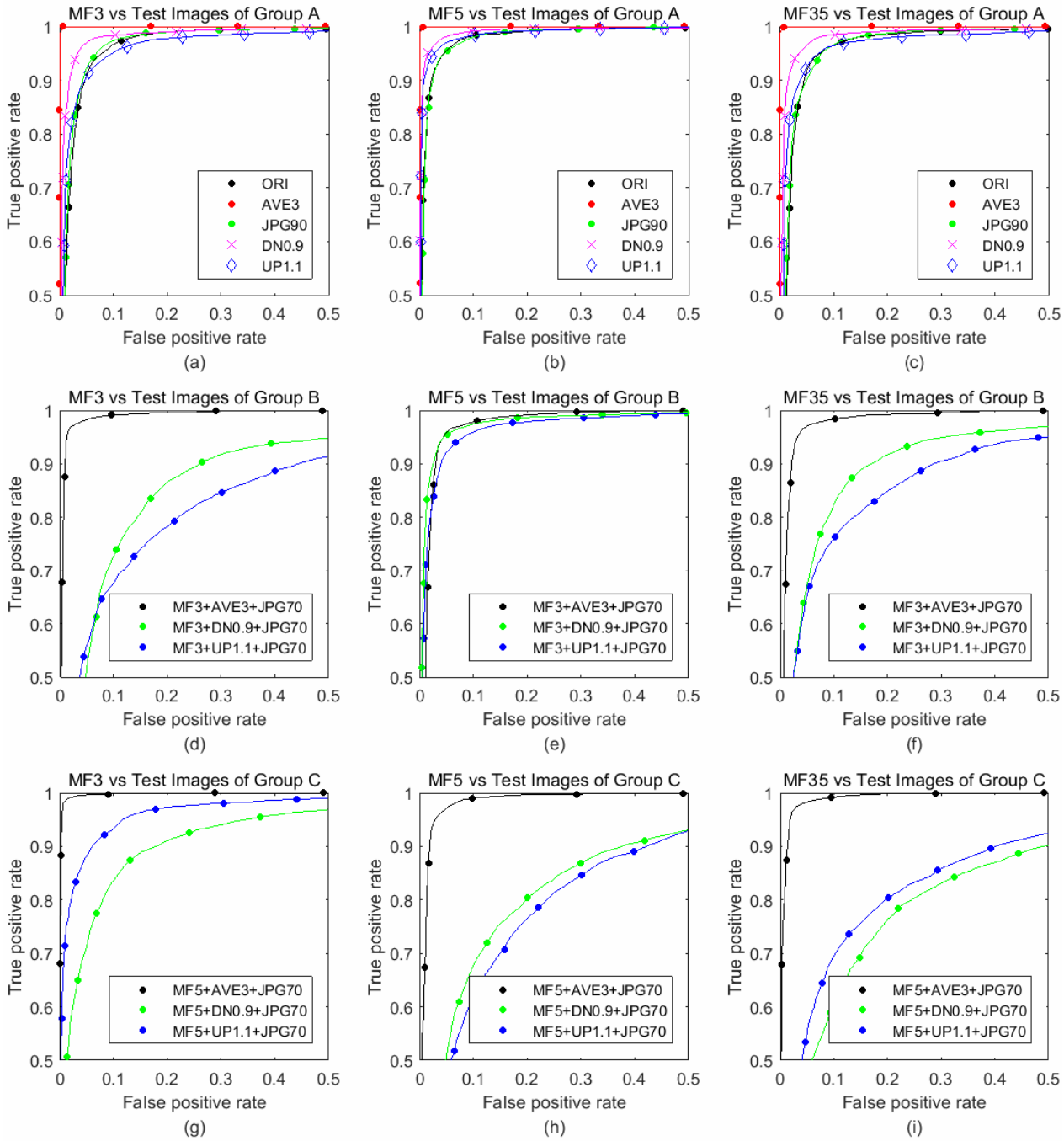

Fig. 7. ROC curves of the proposed MF detection scheme.

• Group B: Post-altered two times more, after MF3.
- MF3+AVE3+JPG70
- MF3+DN0.9+JPG70
- MF3+UP1.1+JPG70

• Group C: Post-altered two times more, after MF5.
- MF5+AVE3+JPG70
- MF5+DN0.9+JPG70
- MF5+UP1.1+JPG70

Fig. 5 presents the average AR coefficients of the 'A' group images.

In Fig. 6, ROC curves show each performance on MF*w* versus test images under the MFR [6] scheme, and in Fig. 7, ROC curves show each performance on the MFs versus test images on the proposed MF detection scheme.

Table 1 shows the experimental results of the MF*w* and test image types on AUC and P_e (the minimal average decision error) under the assumption of equal priors and equal costs [13] and classification ratio, respectively.

$$P_e = \min\left(\frac{P_{FP} + 1 - P_{TP}}{2}\right) \tag{14}$$

The above procedure was repeated 30 times to reduce performance variations caused by different selections of the training samples. The detection accuracy, which is the

Table 1. Performance comparison between the MFR and the proposed MF detection scheme.

MF*w*: Median filtering window size, $w \in \{3,5,35\}$
RI(Result Item) 1: AUC, 2: P_e and 3: Classification ratio
A a: ORI
b: AVE3
c: JPG90
d: DN0.9
e: UP1.1
B a: MF3+AVE3+JPG70
b: MF3+DN0.9+JPG70
c: MF3+UP1.1+JPG70
C a: MF5+AVE3+JPG70
b: MF5+DN0.9+JPG70
c: MF5+UP1.1+JPG70

MF Detection Scheme	MF*w*	RI	*A*					*B*			*C*		
			a	b	c	d	e	a	b	c	a	b	c
MFR	MF3	1	0.96	0.98	0.98	0.97	0.99	1.00	1.00	1.00	1.00	1.00	1.00
		2	0.09	0.06	0.07	0.07	0.03	0.00	0.01	0.00	0.00	0.00	0.00
		3	0.90	0.89	0.92	0.90	0.95	0.97	0.99	1.00	0.98	0.98	0.99
	MF5	1	0.84	0.96	0.88	0.87	0.97	1.00	1.00	1.00	1.00	1.00	1.00
		2	0.21	0.09	0.17	0.19	0.07	0.00	0.01	0.00	0.00	0.00	0.00
		3	0.68	0.84	0.71	0.69	0.92	0.99	0.97	0.99	0.99	1.00	1.00
	MF35	1	0.85	0.95	0.90	0.88	0.97	1.00	1.00	1.00	1.00	1.00	1.00
		2	0.21	0.09	0.17	0.18	0.07	0.00	0.01	0.00	0.00	0.00	0.00
		3	0.81	0.83	0.75	0.84	0.94	0.98	0.97	0.99	0.99	0.99	0.99
Proposed Scheme	MF3	1	0.98	1.00	0.98	0.99	0.97	0.99	0.89	0.86	1.00	0.93	0.97
		2	0.06	0.00	0.05	0.03	0.06	0.02	0.15	0.19	0.01	0.12	0.07
		3	0.93	0.99	0.93	0.96	0.95	0.95	0.83	0.84	0.97	0.88	0.89
	MF5	1	0.99	1.00	0.99	0.99	0.99	0.98	0.98	0.98	0.99	0.87	0.85
		2	0.04	0.00	0.04	0.03	0.03	0.04	0.04	0.06	0.03	0.18	0.20
		3	0.95	1.00	0.95	0.98	0.97	0.92	0.96	0.94	0.93	0.84	0.79
	MF35	1	0.97	1.00	0.98	0.99	0.98	0.99	0.93	0.90	0.99	0.84	0.87
		2	0.05	0.00	0.06	0.04	0.05	0.03	0.12	0.16	0.02	0.21	0.18
		3	0.93	0.99	0.92	0.96	0.94	0.93	0.88	0.89	0.95	0.82	0.84

arithmetic average of the true positive (TP) rate and true negative (TN) rate, was averaged over 30 times in random experiments [9].

From Table 1, it can be seen that the performance of the proposed scheme is excellent with MF3, MF5 and MF35 versus ORI, AV3, JPG90, DN0.9 and UP1.1 images compared to the MFR scheme. For the forged image that was post-altered two times more with AVE3, DN0.9, UP1.1 and JPEG70 after MF3 and MF5, the performance of the scheme is lower than the MFR scheme. In particular, the feature vector in this paper has a superior classification against AVE3.

However, in the measured performances of all items, AUC by 'sensitivity' (TP) and '1-specificity' (FP) was achieved closer to 1. Thus, it was confirmed that the grade evaluation of the proposed algorithm can be rated as '*Excellent* (*A*)'.

In all the above experiments, the proposed MF detection considered only AR coefficients of the image line's gradients to form the feature vector in the spatial domain.

5. Conclusion

This paper proposes a new robust MF detection scheme. From an AR model of an image pixel's gradients, the scheme uses the AR coefficients as MF detection feature vectors. The proposed MF detection scheme is compared to the MFR [6], so these results will serve as further research content on MF detection.

This appears to be the complete solution of an AR model from gradients of the neighboring row and column lines in a variety of images. However, despite the feature vector of the proposed MF detection scheme having a short length, the performance results are excellent due to AUC, the classification ratio is more than 0.9, and P_e is closer to 0.

Future work should consider a performance evaluation of smaller sizes, such as 64×64 or 32×32 of an altered image, which were not considered in this paper.

Finally, the proposed approach can also be applied to solve different forensic problems, like previous MF detection techniques.

Acknowledgement

This research was supported by the Ministry of Trade, Industry and Energy (MOTIE), KOREA, through the Education Program for Creative and Industrial Conver-

gence. (Grant Number N0000717)

References

[1] Kang Hyeon RHEE, "Image Forensic Decision Algorithm using Edge Energy Information of Forgery Image, " *IEIE, Journal of IEIE*, Vol. 51, No. 3, pp. 75-81, March 2014. Article (CrossRef Link)

[2] Stamm, M.C., Min Wu, K.J.R. Liu, "Information Forensics: An Overview of the First Decade," *Access IEEE*, pp. 167-200, 2013. Article (CrossRef Link)

[3] Kang Hyeon RHEE, "Forensic Decision of Median Filtering by Pixel Value's Gradients of Digital Image," *IEIE, Journal of IEIE*, Vol. 52, No. 6, pp. 79-84, June 2015. Article (CrossRef Link)

[4] Kang Hyeon RHEE, "Framework of multimedia forensic system," *Computing and Convergence Technology (ICCCT), 2012 7th International Conference on*, *IEEE Conf. Pub*., pp. 1084-1087, 2012. Article (CrossRef Link)

[5] Chenglong Chen, Jiangqun Ni and Jiwu Huang, "Blind Detection of Median Filtering in Digital Images: A Difference Domain Based Approach," *Image Processing, IEEE Transactions on*, Vol. 22, pp. 4699-4710, 2013. Article (CrossRef Link)

[6] Xiangui Kang, Matthew C. Stamm, Anjie Peng, and K. J. Ray Liu, "Robust Median Filtering Forensics Using an Autoregressive Model," *IEEE Trans. on Information Forensics and Security*, vol. 8, no. 9, pp. 1456-1468, Sept. 2013. Article (CrossRef Link)

[7] H. Yuan, "Blind forensics of median filtering in digital images," *IEEE Trans. Inf. Forensics Security*, Vol. 6, no. 4, pp. 1335–1345, Dec. 2011. Article (CrossRef Link)

[8] Tomáˇs Pevný, "Steganalysis by Subtractive Pixel Adjacency Matrix," *Information Forensics and Security, IEEE Transactions on*, Vol. 5, pp. 215-224, 2010. Article (CrossRef Link)

[9] Yujin Zhang, Shenghong Li, Shilin Wang and Yun Qing Shi, "Revealing the Traces of Median Filtering Using High-Order Local Ternary Patterns," *Signal Processing Letters, IEEE*, Vol. 21, pp. 275-279, 2014. Article (CrossRef Link)

[10] G. Cao, Y. Zhao, R. Ni, L. Yu, and H. Tian, "Forensic detection of median filtering in digital images," *in Multimedia and Expo (ICME)*, 2010, Jul. 2010, pp. 89–94, 2010. Article (CrossRef Link)

[11] S. M. Kay, *Modern Spectral Estimation: Theory and Application*, Englewood Cliffs, NJ, USA: Prentice-Hall, 1998.

[12] Article (CrossRef Link) (2015.4.1)

[13] M. Kirchner and J. Fridrich, "On detection of median filtering in digital images." *In Proc. SPIE, Electronic Imaging, Media Forensics and Security II*, vol. 7541, pp. 1–12, 2010. Article (CrossRef Link)

Kang Hyeon RHEE graduated and received a BSc and an MSc in Electronics Engineering from Chosun University, Korea, in 1977 and 1981, respectively. In 1991, he was awarded a Ph.D. in Electronics Engineering from Ajou University, Korea. Since 1977, Dr. Rhee has been with the Dept. of Electronics Eng. and School of Design and Creative Engineering, Chosun University, Gwangju, Korea. His current research interests include Embedded System Design related to Multimedia Fingerprinting/Forensics. He is on the committee of the LSI Design Contest in Okinawa, Japan. Dr. Rhee is also the recipient of awards such as the Haedong Prize from the Haedong Science and Culture Juridical Foundation, Korea, in 2002 and 2009.